

SeeSaw: interactive ad-hoc search over image databases

Oscar Moll
orm@csail.mit.edu
MIT CSAIL
Cambridge, MA, USA

Sam Madden
madden@csail.mit.edu
MIT CSAIL
USA

Manuel Favela
mfavela@mit.edu
MIT
Cambridge, MA, USA

Vijay Gadepally
vijayg@ll.mit.edu
MIT Lincoln Laboratory
USA

ABSTRACT

As image datasets become ubiquitous, the problem of ad-hoc searches over image data is increasingly important. In particular, many tasks, such as constructing datasets for training and testing object detectors, require finding ad-hoc objects or scenes within large image datasets. Existing approaches for searching image datasets rely on rigid categories or assume fully accurate models trained on the data are available ahead of time. In contrast, SeeSaw is a system for interactive ad-hoc searches in image datasets that does not assume a pre-defined set of categories in advance. SeeSaw users can start a search using text, and then provide feedback to SeeSaw in the form of box annotations on previous results. Using this input, SeeSaw refines the results it returns to help users locate images of interest in their data. Behind the scenes, SeeSaw uses several optimizations to transform the user’s feedback into better results. We evaluate SeeSaw against a state of the art baseline that does not take advantage of user feedback and find SeeSaw can increase search quality metrics up 4x for the harder search queries, and significantly on almost all queries, even those where the baseline performs well.

PVLDB Reference Format:

Oscar Moll, Manuel Favela, Sam Madden, and Vijay Gadepally. SeeSaw: interactive ad-hoc search over image databases. PVLDB, 14(1): XXX-XXX, 2023.
doi:XX.XX/XXX.XX

PVLDB Artifact Availability:

The source code, data, and/or other artifacts have been made available at <https://github.com/orm011/seesaw>.

1 INTRODUCTION

Increasingly inexpensive cameras and storage make it ever easier to collect images and video. In addition to dedicated cameras, video and images are now captured from mobile phones, vehicle cameras and drones. At the same time, machine learning based computer vision techniques continue improving significantly – enabling better automation of tasks involving image content understanding. Nevertheless, the ability of an engineer or team to explore their

own data and discover ad-hoc items of interest lags far behind their ability to collect that data. For example: an engineer at an autonomous vehicle company with a large repository of data may wish to find examples of bikes in the snow to test and improve an existing bike detector; a mobile app developer may want to develop a hot-air balloon detector as part of a new app feature; or an ornithology expert may want to search their camera archives to know which of all their camera locations seem to show more sightings of a particular bird. For any of these scenarios, whether training or extending a computer vision model on one’s own data or improving testing for an existing model, the first step is finding at least a few tens of images within the data that contain examples of interest. Depending on the dataset, bikes in the snow and hot air balloons may be quite rare, perhaps appearing in only one in a thousand images or less. In such scenarios, random sampling is unlikely to help these users, and pre-trained object detectors are unlikely to be available due to the rare nature of the query and to differences between the user’s data and the data used to train existing object detectors. Existing consumer image search tools such as Google could be helpful in principle but are not able to carry out searches in the user’s own datasets. Other services such as Google Photos and Apple Photos help users search their own datasets, but are limited in the types of searches they support, and provide recourse for users to fine-tune results when they fail.

To address these challenges, we built SeeSaw. SeeSaw comprises a graphical search UI and server backend that enables users to carry out ad-hoc interactive image searches within their own datasets starting from a text query. SeeSaw does not require any data labelling ahead of time, only a pre-processing step done once over the data to compute image embeddings. Then, given an input query, SeeSaw uses a state of the art visual-semantic embedding model (CLIP [19]) produce an initial set of images. Users can provide SeeSaw with localized feedback about those results which SeeSaw uses to refine query results in real-time and produce a better next batch, which the user can provide feedback on again, etc.

SeeSaw is especially helpful for situations where state of the art approaches like CLIP fall short for any reason: Such situations are unfortunately inevitable and frequent in the ad-hoc search contexts we described because each dataset is different, and each search need is different as well. Instead, the user and SeeSaw can work in a loop to refine the search online. User feedback in SeeSaw takes the form of box annotations around regions of interest within images, which SeeSaw uses to adapt the next result batch to both the user’s intentions and to the dataset. SeeSaw implements ad-hoc searches by

This work is licensed under the Creative Commons BY-NC-ND 4.0 International License. Visit <https://creativecommons.org/licenses/by-nc-nd/4.0/> to view a copy of this license. For any use beyond those covered by this license, obtain permission by emailing info@vldb.org. Copyright is held by the owner/author(s). Publication rights licensed to the VLDB Endowment.

Proceedings of the VLDB Endowment, Vol. 14, No. 1 ISSN 2150-8097.
doi:XX.XX/XXX.XX

leveraging state of the art visual-semantic embedding models coupled with a novel interactive improvement technique which we call *interactive concept refinement* and a time-tested adaptive resolution optimization that requires no training: *pyramid representations*.

Interactive concept refinement consists of incrementally improving an internal vector SeeSaw uses to represent the ongoing query. This vector is used by SeeSaw to index into the pre-processed images, stored internally as a feature vector, and includes information both from strings used to describe the search and from image examples from user feedback. The *pyramid representation* encodes images as bundles of feature vectors (as opposed to a single vector). Each vector within that bundle corresponds to a square box within its image. The pyramid representation assembles vectors of different sizes centered at different spatial locations within the image, allowing SeeSaw to return results where the object of interest occupies only a small portion of the image, as is the case in many domain-specific search tasks (e.g., snowy bikes or birds in a forest scene.). While image-pyramid representations in general are a well known technique, one of SeeSaw’s contributions is integrating *Interactive concept refinement* with a vector pyramid representation.

In summary, the contributions of this paper are:

(1) We introduce SeeSaw, a human-in-the-loop system and interface to enable ad-hoc searches over image data. SeeSaw leverages CLIP as a starting point and works with users to improve results interactively without imposing onerous pre-requisites in terms of labeled data or the availability of models pre-trained specifically on the user’s data.

(2) We introduce vector refinement, a way to implement interactive feedback that works well with pre-trained models such as CLIP.

(3) We design and integrate a vector pyramid representation for images, which helps SeeSaw locate objects of interest at different scales at the cost of increasing database size. We leverage a vector store to keep latencies interactive and derive the payoffs.

(4) We evaluate SeeSaw in a randomized user study against a baseline system without optimizations, showing the extra time burden on users is low, but the gains in time and results can be large (3x) especially for rarer or more complex situations.

(5) We demonstrate SeeSaw adds substantial value to state of the art models such as CLIP when used for image search over several well known datasets such as COCO, LVIS and BDD. Our benchmarks show improvements of 3.1x in NDCG score (a retrieval metric) on cases where the model performs poorly, while not hurting accuracy when it performs well on its own. We show substantial improvements across all data sets.

2 VISUAL-SEMANTIC EMBEDDINGS

Before describing SeeSaw in detail, we introduce visual-semantic embedding models, a special kind of embedding used as a building block for SeeSaw. A visual-semantic embedding model consists of two models, one for a visual data modality and one for textual modality. A visual embedding model that converts images to vectors, and a language embedding model that converts sentences to vectors. In a visual-semantic embedding model, the two constituent models are jointly trained on a corpus of captioned images so that corresponding images and captions are mapped by the image embedding and language embedding respectively into two vectors

with high cosine similarity, while non-corresponding image, vector pairs should map to two vectors with low cosine similarity. In this way, both images and text are mapped into a common ‘semantic’ vector space which is useful as a high-level representation. For image search tasks, the visual part of the visual-semantic embedding can be used without needing any text just like a pure image embedding, the text was only used during training. The advantage now is that at query time the user can convert their a search query string into a vector using the language model, and use that vector to locate image vectors with a high cosine similarity from a database. One example of an openly available state-of-the-art visual-semantic embedding is CLIP[19]. CLIP is pre-trained on a large corpora of web images and captions.

Frameworks such as [21] help users potentially build their own embeddings. Training your own multi-modal embedding requires a captioned corpus for training, requiring users to caption their data would impose the kind of barrier to getting started that we want SeeSaw to avoid. Luckily, pre-trained visual-semantic embedding on large language-image datasets from a web crawl have been shown to have competitive predictive performance on datasets they were not trained on [19], raising the possibility that such models could be used even in custom domains. However, [19] also find performance can lag behind domain-specific pre-trained models, and performance can drop for other domains. Nevertheless, models such as CLIP provide a better search starting point than random search or object detectors, making ad-hoc searches more feasible.

Using a single model as a standalone solution suffers from multiple drawbacks. The first three are due to model limitations and the fourth is an interface limitation. Model limitations are that accuracy of searches using CLIP can vary dramatically depending on the queries and datasets: some queries in some datasets perform almost perfectly, returning mostly positive results in the top 10, some others can perform quite poorly. The second is that search accuracy is somewhat sensitive to the precise search terms used: language models are not magical, and changing the wording can change the top results even if the meaning should be about the same. The third is that models can be somewhat sensitive to changes in object sizes across datasets. This is a big deal if image sizes also change. It is not clear ahead of time for which queries and datasets these issues will be significant. The interface limitation is that even if we have access to a ‘perfect’ visual-semantic embedding, a search string is only able to capture part of what the user has in mind. The human-in-the-loop approach embodied in SeeSaw helps users get started with their searches immediately and address these types of problems if and when they arise, and only for use cases important to them. In cases where model performance alone is already high, SeeSaw does not harm result quality. In section §5 we compare SeeSaw against a baseline built using the pre-trained embedding alone. We now explain how SeeSaw is implemented and where visual semantic embedding models are used within SeeSaw.

3 SYSTEM

SeeSaw consists of the following components: 1) a graphical user interface (GUI), 2) a visual semantic embedding, 3) a vector store, and 4) an optimizer layer.

Before using SeeSaw, we require a one-time pre-processing pass over the user data. Pre-processing in SeeSaw consists of converting raw image data into semantic feature vectors using a pre-trained

visual embedding. For SeeSaw, the runtime of this preprocessing pipeline depends on four variables: the number of images in the dataset, the pixel sizes of the images in the dataset, the inference cost of the embedding, and the number and type of GPUs available. On COCO, a dataset of 120000 images, SeeSaw preprocessing in our unoptimized single GPU pipeline took less than 3 hours.

After preprocessing, users interact with SeeSaw through the SeeSaw GUI. A user wishing to make a model to detect hot-air balloons can begin the search process with SeeSaw through text by typing 'hot-air balloon' into the search box. SeeSaw translates this 'hot-air balloon' string into a semantic vector representation w suitable for lookup into a vector store holding the feature vectors computed during preprocessing. One of SeeSaw's contributions is its optimizer: a layer that generates better and better w as the search progresses. We explain the optimizer in full detail in §4. Given the optimized vector w SeeSaw queries the vector store for high scoring vectors. Scoring vectors is done via dot product: a vector v in the database is considered relevant if $w \cdot v$ is large. The vector store returns a list of high scoring vectors, and the SeeSaw optimizer applies some modifications to this list. The user then sees the corresponding images in the UI.

The user can continue the search by providing feedback on the results offered so far. The flow of data for both preprocessing and interaction is show in Figure 1.

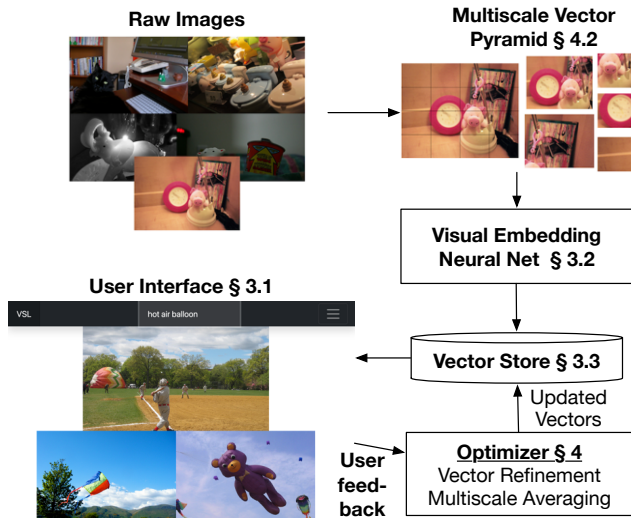


Figure 1: SeeSaw component diagram. Top: preprocessing steps; Bottom: dataflow during interaction loop.

The optimizer layer encapsulates the main research contributions of SeeSaw, and we explain it in detail in §4. The remainder of this section describes the other SeeSaw components briefly.

3.1 User interface

Figure 1, bottom left, shows a screenshot of the SeeSaw UI for the hot air balloon query as one of the components of SeeSaw. The UI receives user input in the form of text or an example image (which could be from outside the database). The UI displays search output images, and accepts further user feedback in the form of bounding box annotations to highlight relevant parts of an image.

3.2 CLIP

SeeSaw employs CLIP[19], a pre-trained visual semantic embedding during both preprocessing and during querying. CLIP was used off-the-shelf, without any access to the data used for the evaluation, because we are interested in the common scenario of lacking labelled data (in this case, lacking a set of captioned images). During pre-processing SeeSaw uses the visual component of CLIP to convert unlabelled images into vectors. During querying, SeeSaw uses the text component of CLIP to handle translation of string inputs from the user.

The vectors produced by the text embedding could be used directly to query the vector store, but SeeSaw instead inputs them to the vector optimizer, which allows SeeSaw to improve the quality of lookups into the vector store. Similarly, SeeSaw does not use a single-vector representation as suggested above, instead uses a multi-vector representation described later.

3.3 Vector store

After data is preprocessed, the vector store provides a key-value lookup interface. The vector store takes a vector w as the key for a lookup and a number of desired results h , and its outputs are h vector ids for vectors v found within the database such that $w \cdot v$ are the h highest. In SeeSaw, the vectors in the store correspond to images in the dataset, but not in a one image-to-one vector manner. Instead, as we explain in §4.2, SeeSaw stores multiple vectors per image corresponding to different image patches at different scales. The vector store does not need to be exact, and for the current implementation we use the Annoy vector store [4].

4 OPTIMIZER

The optimizer encapsulates the core contributions of SeeSaw. It integrates *interactive concept refinement* and *vector pyramid representation*. At a high level, interactive concept refinement enables SeeSaw to improve the quality of results during the course of a user search by leveraging interactive user feedback. The vector pyramid representation enables SeeSaw to greatly increase accuracy on queries of objects that show up at different scales across images, as well as handle images of different sizes. Both optimizations can be deployed independently of each other, but they also can be adapted to work well together. We explain interactive concept refinement in §4.1 and the vector pyramid representation in §4.2.

4.1 Interactive concept refinement

Before describing the concept refinement optimization we first define more clearly what we mean by concept. A *concept* is meant to represent a scene type, an object type, or a situation that can be recognized by a user within an image. For example, a hot-air balloon is a concept, and so is partially cloudy weather, and so is a person riding a bicycle. To allow maximum flexibility in our definition of concept we define a concept formally to simply be a subset of images within our database. For a hot-air balloon, the concept is the set of images containing a hot-air balloon somewhere. We will use S to denote the set of images corresponding to a concept. Note that in this discussion we make a distinction between the concept S , and the text input 'hot-air balloon'. S is the result set, while the text 'hot-air balloon' is just a string we can feed into SeeSaw. We can

also use the text ‘hot air balloon’ without a dash, etc. We assume the universe of images is the set of images in the database. A user search involves SeeSaw working with the user to find images in S . Concept refinement is the process of using user inputs and feedback to find elements of S .

Once images are converted into vectors during preprocessing and loaded into a vector store, we can think of the concept S as a set of vectors or as a set of images interchangeably. For the purposes of our exposition of concept refinement in this section we will make a simplifying assumption and treat images and feature vectors as corresponding one-to-one with each other. This one-to-one assumption will be relaxed in section §4.2 when we explain the vector pyramid representation that associates multiple vectors with a picture, and we will address the system-wide changes needed then. In the following discussion, assume all vectors are normalized to length 1.

In order to support search operationally over a database of vectors, we rely on finding a function F_S such that $F_S(v) > F_S(v') \forall (v \in S, v' \notin S)$. The ideal function F_S ranks database elements so that all images in the concept set S appear before all images not in the set. SeeSaw aims to help the user approximate F_S interactively. In principle we could approximate S better by using a complex scoring function. SeeSaw opts for assuming there is a good linear model approximation: for every concept S there exists some vector w^* such that for all v in the database, $F_S(v) \approx w^* \cdot v$. We can think of this vector w^* as a weighting of embedding features, as a linear classifier without the bias term (since we only care about relative ordering) or even as an archetype of elements of S because it exists in the same vector space as the database elements. Operationally, all interpretations of w^* mean we can make use of vector stores such as [4], which enable us to approximately find vectors v within the database such that $w^* \cdot v$ is large, without requiring a full database scan. This is important because SeeSaw has no access to the true w^* , instead SeeSaw refines an estimate w of w^* and this interactive refinement requires multiple look-ups into the database within a single user search session.

So, for a given concept S , we want to find w such $w \cdot v$ is largest for $v \in S$ and lowest for $v' \notin S$. We would like in fact for $w \cdot v > w \cdot v' \forall v \in S, v' \notin S$ but this ideal vector is not guaranteed to exist: it depends on both the quality of the vector representation (which depends on the pre-trained embedding model) and the distribution of elements concept S within the database, as well as the distribution of its complement set. However, some w 's will be better than others. For instance, there is always at least some w that minimizes the number of out-of-order pairs in the sort order implied by scores. This number is given by the function:

$$L_{\text{inversions}}(w) = \sum_{(v \in S, v' \notin S)} \llbracket w \cdot v \leq w \cdot v' \rrbracket \quad (1)$$

where $\llbracket \cdot \rrbracket$ is an indicator function with value 0 when the enclosed condition is false and value 1 when it holds true. For a given S , SeeSaw helps the user approximate w by allowing them to provide string descriptions, image hints, and interactive feedback from previous results. The process of improving w interactively is what we call interactive concept refinement and one of the main objectives

of the optimizer layer in SeeSaw. We now introduce the techniques SeeSaw provides for interactive concept refinement.

4.1.1 Estimating w^* . In principle, given a random sample of labeled vectors from the database we could estimate w^* much like learning a linear classifier. We can use many continuous loss functions to approximate the number of order-inversions of Equation 1 (which has a discontinuity at 0); for SeeSaw we used a hinge-loss based function as in [10]:

$$L(w) = \sum_{v \in S, v' \notin S} \text{relu}(wv' - wv) \quad (2)$$

Where relu is the rectified linear function and $\text{relu}(wv' - wv)$ is a hinge loss approximating the inversion indicator function used in Equation 1: $\llbracket wv' \geq wv \rrbracket = \llbracket wv' - wv \geq 0 \rrbracket$.

We can minimize L to find an estimate \hat{w} :

$$\hat{w} = \arg \min_w L(w) \quad (3)$$

The formulation of Equation 3 using loss Equation 2 can only be used directly with a sample containing at least one labeled positive and one labeled negative example. However, in SeeSaw we do not have any examples at the start, and finding the first positive example is itself not expected to happen within several tens of pictures if we use random sampling: the cases for which search is most useful are those for which examples occur rarely in the database, those for which random sampling would not work very well. For example, in our evaluation we include some classes with examples appearing in 1/1000 of the images. We want SeeSaw to be useful even when concepts do not appear often in the data.

4.1.2 Finding the first positive example. SeeSaw lets users start their searches with a string description of what they are looking for. SeeSaw relies on the pre-trained visual semantic embedding model to map the search string into a vector w_s . w_s is used as an initial approximation of w^* and SeeSaw queries the vector database with it. The quality of w_s as an approximation of w^* depends on several factors: the embedding model, the dataset, the exact string s used to make the query (‘hot-air balloon’ vs ‘hot air balloon’ without a dash). In our experiments we find using w_s is generally better or than random sampling even though the visual-semantic embedding was not trained on the datasets used in the evaluation.

4.1.3 Finding the second positive example. Suppose the user looking for hot-air balloons and searches with string ‘hot-air balloon’, the string is converted to a vector w_s by the visual semantic embedding and matched against the vector store. The top 20 results include 1 image with a hot-air balloon with vector u in it and 19 without it. There are less than 5 hot-air balloons in the dataset per 1000 images (something the user does not know) so w_s was already much more effective than random sampling. The user provides feedback about this positive example to SeeSaw by marking the hot-air balloon image as a positive. The rest are marked negative.

How should SeeSaw search for the next 10 results? SeeSaw could ignore the feedback and query the vector store with w_s again. After all, w_s already worked once. Alternatively, SeeSaw could use the example u as a query vector now. Alternatively, SeeSaw could use both the positive and negative examples from this first round to generate a third option \hat{w} by solving the optimization problem in

Equation 3 with vectors from this first batch of results. The right choice depends on which is more accurate, which we do not know ahead of time.

Empirical results in [19] and elsewhere, and also in the datasets used in our evaluation show linear models trained on even just one or two positive examples can achieve high accuracy (compared to random). This suggests \hat{w} is a good candidate to use despite a small number of training examples. However, switching from w_s to \hat{w} after we find our first result can result in large accuracy drops on subsequent rounds because while the accuracy of \hat{w} increases quickly as we observe more examples, the accuracy of w_s can be already quite high at the start.

SeeSaw approaches this dilemma with the following principle: 1) we improve w iteratively using gradient descent steps guided by the loss function of Equation 3 2) we incorporate prior information such as the string hint w_s as a starting value in our iterative update. A gradient descent step is defined as:

$$w' = w - \eta \nabla_w L \quad (4)$$

Where η is a learning rate hyper-parameter which we will address later on. To apply a gradient step we require a starting w . For a convex function of w (which the loss L defined in Equation 2 is) this point can be picked at random and the algorithm will eventually converge to the optimum. In SeeSaw, we will use w_s not only to find the first examples, but also as our starting point for taking gradient steps, treating w_s as a good starting guess. This choice does not affect the eventual convergence but in cases where w_s is better than random we start the search closer to the optimum. We should note that in practice we expect SeeSaw users to care most about whether SeeSaw improves results within the first handful of iterations, so the eventual convergence is not the main goal. In our evaluation we only consider the first 10 iterations of the update algorithm and we find this update rule shows substantial improvements to the quality of results compared to using only w_s even within that short number of steps.

We can derive an explicit update rule for w by applying the definition of gradient to the loss L from Equation 2 with respect to w , which yields:

$$\nabla_w L = \sum_{v \in S, v' \notin S} \llbracket w^\top v' \geq w^\top v \rrbracket (v' - v)$$

Where $\llbracket \cdot \rrbracket$ is an indicator function as explained before. Using that formula we can rewrite the gradient step to:

$$\begin{aligned} w' &= w - \eta \sum_{v \in S, v' \notin S} \llbracket wv' \geq wv \rrbracket (v' - v) \\ &= w + \sum_{v \in S} \eta |\{v' | v' \geq_w v\}| \cdot v - \sum_{v' \notin S} \eta |\{v | v' \geq_w v\}| \cdot v' \end{aligned} \quad (5)$$

$|\{v' | v' \geq_w v\}|$ is the number of negative vectors v' appearing higher in the ranking than the positive vector v . This update rule has two intuitively desirable properties: 1) the updated vector w' is a weighted sum of the previous query vector w and the observations so far. The new vector w' moves closer to observed positive examples v and away from the negative ones v' . The relative weights of each example in this sum are based on the amount of error in

the current ranking quantified by the number of mis-ranked examples relative to each vector. When the initial search vector w_s turns out to be a good approximation for our concept S , w will not change much. When SeeSaw finds a positive example v buried late in the results, SeeSaw gives that example a higher weight making the value of the next w be more similar to v than if it were placed earlier in the results.

Now we move on to our choice for hyper-parameter η . We tuned η to a value of 0.005, and we normalize the vectors v and w_s to unit length. Intuitively we know low η results in very little change on each iteration (performing much like w_s), while a high η results in quickly forgetting the original w_s . We do not propose a theoretically justified method of setting this parameter even with a fixed η picked once, the loss derived weights of Equation 5 adapt naturally to the data and the initial guess.

By integrating both the initial guess from the visual semantic embedding and user feedback SeeSaw results are consistently higher in quality than either using only the visual semantic embedding or using only a trained model based on feedback. We now move on to the pyramid representation optimizations in SeeSaw.

4.2 Vector pyramid representation

In this section we describe the vector pyramid representation, the second important optimization in SeeSaw. By pyramid representation we refer to the way we represent images in the system: instead of using a single vector per image, we represent an image with multiple vectors, where each vector corresponds to features extracted at different spatial locations within the image and at a range of different size scales. Pyramid representation causes cross-cutting changes in SeeSaw: it affects not only preprocessing but also the processing of queries and results, and it enables SeeSaw to take advantage of finer grained user feedback through the UI, such as box annotations around regions of interest.

The motivation for this pyramid representation is that state of the art convolutional models are sensitive to pixel sizes of objects within images. During training, most convolutional models learn to recognize objects of a given range of pixel sizes within images of a given pixel size. For example, ImageNet pre-trained feature extractors typically train on square images of size 224x224. The CLIP image-text embedding itself is trained on 224x224 images as well (plus captions). ImageNet images contain objects that fit neatly within that 224x224 box, and which are not much smaller than their containing image. Changes in these statistical properties affect feature extractors: a small decrease in the relative size of objects within that 224x224 pixel window, even if the dataset is otherwise the same, is known to affect ImageNet classifier accuracy [23]. Size decreases are not the only potential problem; for examples [5] points out that for object detectors sometimes it is better to decrease input image size prior to running a pre-trained model, i.e., larger images are not always better.

For datasets in the wild, object sizes and image sizes vary drastically. For example, among the datasets we use in our evaluation, images in the BDD dataset are around 800x1200 pixels. Some objects interest only span a less than 100 pixels, such as dogs, while objects such as Trucks can take almost the full frame. Without requiring annotations ahead of time, SeeSaw does not have a way to know the

sizes of objects that will be queried, The pyramid representation is a scale agnostic preprocessing and query processing strategy, and SeeSaw uses this principle to be able to work on ad-hoc queries over different datasets. We explain how we compute the pyramid representation next in §4.2.1, and then in §4.3 explain how the optimizer integrates with it.

4.2.1 Preprocessing. During preprocessing we aim to extract multiple feature vectors at different zoom levels from the same image. Figure 1 on the center top shows an illustration of pyramid preprocessing. SeeSaw generates a vector for each square ‘patch’ within the image defined by the grid we mentioned above. The intuitive benefits of such a representation are that the vector store includes vectors for patches of different sizes and centered on different points within a single image. The intuitive motivation is that for any arbitrary logical region of an image that turns out to be of user interest during a search, there is at least one patch within the database with a good overlap with the region. For example, the image in Figure 1 shows patches containing a clock as well as a pig. These different patches will score more highly when searching for a clock or a pig respectively than the full image with both objects appearing far less prominently.

The preprocessing algorithm for a single image consists of a downscaling and a tiling stage: In the downscaling stage, given an input image I_0 of size $W \times H$ we generate a sequence of images I_0, I_1, \dots by downscaling each by a factor $r < 1$ (for example $r = 1/2$) successively. This type of image sequence is known as an image pyramid[1]. I_1 has size $rW \times rH$, I_k has size $r^k W \times r^k H$. For SeeSaw, we stop the sequence when the shorter side of I reaches a minimum size z . The exact minimum size limit depends on what the embedding can handle (which depends on how it was trained). We use size $z = 224$ because CLIP expects images of that size. For our evaluation we use $r = 1/2$ but it is possible a larger r could be a better choice.

For the tiling stage each image in the pyramid I_0, I_1, \dots is logically divided into tiles of size $z \times z$ and each tile is then mapped to a vector using the embedding model. Instead of disjoint tiles we use a strided tile pattern to have partial overlap between tiles: the next tile of size z starts at offset $z/2$ from the start the previous tile.

When tiled in this manner, each element of the pyramid generates multiple vectors and each vector corresponds to a 224×224 tile in their respective image I_i . This tile in I_i logically corresponds to a larger tile of side $224/r^i$ in the original image I_0 . For each vector generated in this stage we store the vector’s corresponding box metadata (x_1, y_1, x_2, y_2) in pixel coordinates with respect to I_0 . This box metadata will be helpful later on during query processing to understand the relations between vectors on the same image.

An image of size $W \times H$ maps to approximately $\frac{W}{z/2} \times \frac{H}{z/2}$ vectors after tiling. Because of the multiplicative size decrease going from I_i to I_{i+1} , for $r < \sqrt{1/2}$ more than half of the vectors will come from patches in I_0 . We will refer to I_0 as the *base* or base level of the pyramid, as it employs a larger image and produces the most vectors (much like the base of a pyramid is the widest part). We will refer to the last I_k in the sequence as the *top* or top level of the pyramid. A 1200×800 pixel image maps to around 100 vectors. As mentioned in §3, pyramid preprocessing for the 120k image COCO dataset on an unoptimized 1-GPU pipeline takes less than 2

hours. In our evaluation we find this overhead is compensated for in result quality. We also note that the user can ultimately change the r parameter, and could decide to skip the lowest pyramid level if one is only interested in larger areas. In principle, extra levels can also be added over time if desired.

We have described how preprocessing works in SeeSaw to generate the pyramid feature representation, but changing this representation also involves changing how we process queries, which we explain next.

4.3 Integrating vector pyramid with optimizer

This section explains how we integrate the pyramid representation computed during pre-processing into the optimizer at query time. Upon receiving a user string query to start a search, SeeSaw converts that query into an initial query vector w_s using the visual-semantic embedding. SeeSaw uses w_s as a key to the vector store, and obtains a list of the top- l vector ids (those for which $w \cdot v$ is maximized). Unlike before, these vector ids no longer correspond one-to-one with images. Instead, they correspond to individual vectors within the pyramid representation of images. The most immediate approach to convert a rank of vectors into a rank of images is to rank image ids based on the maximum score from among all of the vectors in its pyramid. This approach makes some intuitive sense because we want to return results even if they do not occupy a large area within the images we are searching: in those cases, we expect only some parts of the image will have high scores while the unrelated parts of the image may not, and that should not affect the overall score. This approach can be implemented using the vector store to retrieve l results, with l large enough so that there are vectors for at least k different images. Then, we group these l scores by image and find the max per image. Indeed, we find that this strategy helps improve quality for many queries. Unfortunately, we find this strategy also hurts accuracy for many queries. The reason for this unexpected drop is that max-scoring the pyramid representation increases scores for positives, but also creates an increase in high-scoring negatives: the maximum numerical scores for any lookup key w tends to increase at the base level of the pyramid regardless of actual relevance. There are multiple ‘failure modes’ we notice in the data that explain this phenomenon, including:

Meaningless patches at base of the pyramid: or example the center top of Figure 1 shows three base level patches for an image. Two of them include recognizable objects but one includes a piece of wall. Such patches are hard for humans to interpret without context, and seem to also be hard for the embedding to interpret correctly.

‘Lookalike’ patches: shapes resembling objects being queried for that however are clearly not the objects (for a human). Examples of these include parts of wooden sticks being confused for baseball bats, for example a patch with only the leg of a wooden chair. We use these observations to address the accuracy drop in the next section.

4.3.1 Multiscale averaging. How can we separate the good patch results from this type of noise we added? SeeSaw addresses this problem by leveraging the redundancy built into the pyramid patch scheme and using it to re-score each image. We find these hard-negatives for many queries tend to score low when we score at them at different scales, but happen to score high at the base scale

of the pyramid. In contrast, true positives for many queries tend to be more stable in scores across at least a few of the scales. We leverage this empirical observation to implement a type of multi-scale averaging: each of the l vectors in the list from the vector store corresponds to a patch in an image. Within a single pyramid representation, for any given patch in the database there are multiple overlapping patches at different scales that also have a view of a similar area. We can use these other patches to judge the reliability of the vector score. For each vector v in the shortlist we retrieve other vectors from the database purely based on the spatial overlap with v . In our current implementation we use the box metadata for each vector to compute the list of other vectors that maximally overlap with v when measured using the intersection over union of their corresponding boxes, and then we average the scores of these overlapping vectors for the same w . Note that these overlapping vectors need not be in the l element shortlist. This new adjusted score is used to re-rank the images we show the user: we show the k images with the top adjusted scores. Because we rely on the re-ranking to move hard-negatives to the bottom of the list and to surface k positives, we want l to be multiple times larger. Currently we set $l = 10 \times k$. We find multiscale averaging followed by reranking results helps improve accuracy for most queries, including queries for small and for large types of objects.

4.3.2 Fine-grained feedback and refinement with a vector pyramid representation. The pyramid representation also affects the way users provide feedback and the way SeeSaw takes advantage of it. When SeeSaw shows a list of k images to a user, the user marks specific regions of interest within the image as positive using a drawing tool built into the UI. SeeSaw integrates this fine grained feedback by mapping back from user drawn regions onto all those vectors in the multi-vector representation that correspond to high-overlap (high IoU) patches (recall each vector in the multi-vector representation was computed from a box-shaped region of the image, and that SeeSaw records this region for each vector). Those vectors can be used as ‘positive’ examples for the refinement introduced in §4.1, while zero overlap vectors are used as negatives. Currently, SeeSaw uses vectors with high overlap with the marked region, and whenever more than one vector from a given zoom level would qualify, we pick the vector with the highest overlap.

Incidentally, because the search process could return more than one vector (but at least one), this search process also provides a type of training-time augmentation. Unlike typical augmentation techniques, this augmentation occurs at low runtime cost, because all vectors have been pre-computed.

5 EVALUATION

The goal of our evaluation is threefold. The first goal is to demonstrate that SeeSaw delivers high quality results across queries from very different datasets spanning web images, aerial/overhead imagery, and vehicle camera imagery and queries of many types of objects and scenes, including relatively rare situations (§5.2). Second, we want to see how well real users can use SeeSaw to perform image search (§5.3). Finally, our third goal is to break down the contributions of the interactive refinement and pyramid representation optimizations to SeeSaw performance (§5.4).

For the first goal, we simulate a SeeSaw interaction with user box annotations for more than a thousand different queries and compare SeeSaw results against a non-interactive baseline using a state of the art visual semantic embedding (CLIP)[19] on its own. Then, in §5.3 we perform experiments with real users searching with SeeSaw, in versions with and without the refinement and pyramid optimizations.

5.1 Experimental Setup

In this section we summarize the datasets and metrics we use in our experiments.

5.1.1 Datasets. We evaluated SeeSaw on the following 5 datasets: **BDD[24]** image frames from a vehicle mounted video camera dataset collected from multiple cities and highways. It includes object annotations for about 12 objects. Frames are of size 1280x720. In addition to object labels, BDD includes global scene attribute labels such as weather (‘cloudy’, ‘snowy’) location (‘highway’, ‘city’, ‘tunnel’, ‘parking lot’) etc. These extend the total number of queries that can be evaluated to around 30 categories. Some objects such as bikes and motorcycles occupy only small pixel areas around 50 pixels in size. Some queries include finer grained attributes, such as ‘yellow traffic light’ or ‘person riding bike’.

COCO[14] a well known object detection dataset, used to train and evaluate state of the art object detectors. COCO includes annotations for 80 classes of objects including indoors and outdoor scenes. Images in COCO were originally pictures collected from Flickr, and so their content, image sizes and aspect ratios vary within the dataset, but most are in the 600-800 pixel range.

LVIS[7] shares the same underlying image set as COCO, but with a highly enriched label set, including labels for a long tail of 1200 classes of objects not present in the original COCO dataset. Most of these classes are much more rare and specific, but not exhaustively labelled.

ObjectNet[2] an object classification dataset with 300 different categories of objects taken deliberately in non-standard angles and backgrounds. Raw images vary in size but the provided labels apply only to the 224x224 centered crop of the image, so we use only that part of the image.

The datasets were chosen to show a range of domains: vehicle dashcam video frames, web images and non-standard images. Additionally, objects in the datasets range in how common they are. LVIS includes classes that appear only up to a handful times in the dataset, so are only present in about .5% of their labelled images and helps evaluate very ad-hoc searches that would be hard to think of ahead of time. BDD includes images relevant to the autonomous vehicle space. BDD images are different from COCO in that they are not taken by a photographer biased to focus and center a specific object within the scene. BDD also includes a lot more complex scenes: frames are relatively large, and there are many instances of objects of different sizes on each image. BDD also includes ‘full scene’ categories which are not just a type of object.

We evaluate each dataset separately as its own database. Because of the large number of categories they label, the LVIS dataset is not exhaustively labelled. For each of the 1200 classes LVIS provides instead an explicitly enumerated subset of images within the dataset where the class is either labelled or confirmed to not be

present. Each of these tends to be of around 1000-2000 images. For each of those classes we run a separate evaluation limited to their corresponding subset of the LVIS image set.

Preprocessing: We ran the SeeSaw preprocessing pipeline on each dataset, with the largest datasets taking under 2 hours on a 2 Volta GPU machine. The largest vector database (BDD) comes to 30GB, and about 100 vectors per image (due to the relatively high resolution of the images), COCO sits in the middle, and ObjectNet being an image classification dataset by design uses 1 vector per image (because image dimensions are 224 x 224).

5.1.2 Benchmark. SeeSaw is meant to be an interactive system where a user begins a search with a text string. Then, SeeSaw returns an initial batch of results of a configurable length (we use size 10 in our experiments). Following that, the user provides feedback on the results by marking those which are correct by drawing boxes around the relevant results. The system uses the information provided thus far to produce a new batch of results for the user to inspect. For our evaluation we simulate this human-system loop by using human annotations of the datasets introduced in §5.1.1. For the initial search string we generally use the category names from each dataset. For the BDD dataset we change category names such as ‘motor’ to a more appropriate textual description: ‘motorcycle’. For LVIS and ObjectNet with 1200 and 300 categories respectively, we programmatically change category names so that the parenthesis and slashes are replaced with spaces. We apply some adjective reordering as well, for example the category ‘book (closed)’ gets converted to ‘closed book’ for querying SeeSaw, ‘eraser (white board)’ is queried as ‘white board eraser’, ‘tablet/ipad’ is queried as ‘tablet or iPad’. The full list of modifications is provided with the source code.

For each query we simulate a loop with 10 search iterations, each showing 10 image results. SeeSaw does not repeat results, so this results in 100 different results for each query. The first iteration follows the initial string search, the following 9 iterations include feedback on all the previous batches. We use dataset provided bounding boxes to simulate user box feedback. There are multiple ways to measure the quality of this sequence of 100 images, which we explain in the next section.

5.1.3 Metric. We want the ranking metric to be sensitive to the ordering in which objects appear in the results because we expect users may want to stop early, and also, we presume users are less likely to continue searching if all initial results are negative. A simple metric would just be to count the raw number of positive results, N , but this lacks this order sensitivity property. The closely related metric (for a fixed k) Precision@ k simply divides N by k . This change by itself does not provide order sensitivity, and creates a second problem. Categories such as hot-air balloon which only have a handful of positive results (5 in total) will never score more than 5% Precision@ k even for a method that returns the 5 hot-air balloons in the dataset as the top 5 results. One way to avoid this problem (and to add order sensitivity) is to switch to the more complex metric AveragePrecision@ k [17] which averages the precision values at different points in the 100 results (corresponding to points with a positive result), stopping the calculation at 100 results. Our hypothetical method that returns the five hot-air

balloons as the top 5 results would score an average precision of 1 because precision at each recall point was 1. However AveragePrecision@ k presents a new dilemma when handling a different method that returns 4 hot-air balloons as the top 4 results and none after: how should the missing hot-air balloon affect the score so that we can compare the two methods? If we ignore it and simply average existing recall points (the first 4 results), we still get an average precision of $4 * 1./4 = 1$, which would be misleading. If we consider the missing example a complete miss, and give it a precision of 0, we get an average precision of $(4 * 1. + 1 * 0.) / 5 = .8$. This score seems reasonable, but has other problems. If we apply this metric to a more common category such as bikes for which there are say 200 positive results we will find that a method with 100 positive results at the top 100 has AveragePrecision@100 using this definition would be .5, which would also be quite misleading, since that ranking is the best we could hope for if we only return 100 results. NDCG [17] (normalized cumulative discounted gain) is an commonly used metric in the information retrieval community that helps address these dilemmas.

NDCG is defined in terms of DCG explained below and a normalization constant. DCG is the weighted sum:

$$DCG(k) = \sum_{i=1}^k \frac{rel_i}{\log_2(i+1)}$$

Here, rel_i is 1 or 0 in our experiments, depending on whether the result contains a relevant object or not. The denominator $\log_2(i+1)$ is an increasing discount that weights earlier results higher. The *normalized* DCG, or NDCG is the above DCG score divided by the score for the best possible ranking for that dataset and the number of results shown to the user $k = 100$ (i.e., the best possible DCG score an oracle could obtain). The NDCG score is 1 for the hot-air balloon example in the case of the top 5 images being the 5 hot-air balloons, and would be slightly somewhere above .8 (later results are weighted less) if only 4 hot-air balloons. NDCG is 1 in the bike example when the top 100 results are bikes. An NDCG score for a result list is 1 if and only if the dataset cannot possibly be ranked better within those 100 results, and an NDCG score is 0 if and only if there are no positives in the top 100 results. An NDCG score of .5 could be due to the total number of positives found being smaller the maximum or the locations of positives not being first in the ranking. In our evaluation we use scikit-learn’s [18] implementation of NDCG.

The normalization step in NDCG helps us handle situations where either the number of true positive results is very low or very large compared to the number of shown results, and lets us better compare across methods that return different total numbers of results in the top k across methods and across different queries.

5.1.4 Baseline. To our knowledge there is currently no system offering the type of interface we describe for image search that we can use as a baseline. Our baseline for evaluation is to process the search using the same high quality pre-trained visual semantic embedding (CLIP) used in SeeSaw to obtain 100 results without user feedback or pyramid representation. Re-scaling and center-cropping images to fit in a 224x224 box is one way to create a one-image-one-vector representation. We found that some images are more of a rectangle than a square, so the cropping sometimes

leaves some objects out completely. We did not want this cropping to affect result metrics, so we modify this process slightly to cope with rectangular images. After the initial re-scaling the shortest side has length 224, and we stride along the long side so that we cover it. We normalize and average these few vectors into a single vector (we normalize before averaging to avoid extraneous length differences affecting scores). This baseline performs better in practice than the rescale-and-crop one, and ensures any differences in results are not due to objects being cropped out.

5.2 Evaluation with Simulated Interaction

In this section we compare the baseline NDCG score with the SeeSaw NDCG score across all queries. Our goal is to quantify SeeSaw search performance in both an absolute and relative way. After running the experiment described in §5.1.2 for each query for both SeeSaw and the baseline, and computing NDCG as described in §5.1.3, we plot a point for every query in our benchmark in Figure 2. The x -coordinate corresponds to the NDCG score of the baseline and the y -coordinate corresponds to the ratio $\text{NDCG}_{\text{SeeSaw}}/\text{NDCG}_{\text{baseline}}$, representing the improvement of SeeSaw over the baseline. We use log-scale for both axes to manage the high variation in the y -axis.



Figure 2: Relative NDCG improvement with SeeSaw vs. baseline for each query in our evaluation. Each point corresponds to a query. The x -axis encodes baseline NDCG and the y -axis encodes $\text{NDCG}_{\text{SeeSaw}}/\text{NDCG}_{\text{baseline}}$. Horizontal dashed lines separate the three areas where $\text{NDCG}_{\text{SeeSaw}}$ is better (top), about the same (within 10% of $y = 1$), or worse than $\text{NDCG}_{\text{baseline}}$ (bottom). Vertical dashed lines separate areas where baseline NDCG is low (left), medium (center) or high (right) initially. A baseline performance of x bounds the maximum possible $\text{NDCG}_{\text{SeeSaw}}/\text{NDCG}_{\text{baseline}}$ value to $y = 1/x$, which we display as a solid diagonal.

A scatter point with $y > 1$ means SeeSaw delivered a better NDCG score than the baseline. Conversely, a scatter point below the $y = 1$ line means the baseline performed better. We draw two horizontal dashed lines, one at $y = 1.1$ and one at $y = .9$ to separate the plot into three horizontal regions: one for queries where SeeSaw performs better, one for queries where SeeSaw performs about equally well as the baseline and one where SeeSaw does not perform

as well. Figure 2 visually shows that the overwhelming majority of queries show improved performance with SeeSaw. We show the actual counts broken down by dataset in Table 1. Table 1 shows out of around 1640 queries, only 40 queries decrease in performance. These queries are spread across the datasets. In every dataset the majority of queries either improved or remained the same. Two of the datasets show no negatively affected queries. ObjectNet shows the most queries remaining the same (relative to improved); part of the reason is that the Pyramid Representation in ObjectNet is not used (all images are already centered and cropped at 224×224). We break down the impact of the different optimization in the next section §5.4.

dataset	better	same	worse	total
bdd	13	13	3	29
coco	23	57	0	80
lvis	764	405	33	1202
objectnet	226	84	3	313
total	1026	559	39	1624

Table 1: Relative change in NDCG relative to the baseline (CLIP) for each query in each dataset. ‘better’ means the NDCG increased for a category by a factor of 1.1 or more and ‘worse’ means it decreased by a factor .9 or less. SeeSaw rarely decreases search result accuracy, and overwhelmingly improves it across each dataset.

The previous analysis quantified the number of queries that improve, but not the magnitude of the improvement, which we discuss next. Figure 2 shows the improvement ratio can exceed 10x on the top left side. The maximum observed improvement decreases toward the right. The curve $y = 1/x$ in Figure 2, appearing as a straight line due to log-log scale, marks the upper bound for possible relative increase in NDCG: if the baseline NDCG is .3 for example, the maximum relative improvement possible is 3.3. The datasets used to evaluate SeeSaw include many queries for which the baseline already performs at levels above .3. SeeSaw’s goal is to help more easily conduct their searches even when the pre-trained embedding model performs poorly initially on their data without negatively impacting results when the pre-trained model already performs well (we do not know which queries will perform well ahead of time). In order to quantify improvements for these different scenarios, we logically partition the x -axis into three vertical regions: those where the baseline NDCG is less than .1, those where it is above .3, and those in between. The areas correspond to ‘low’, ‘high’, and ‘medium’ baseline performance on the query. Figure 2 shows the average improvement clearly depends on this variable, and we quantify the average change in NDCG for each region separately. For each of these vertical regions we average the NDCG scores across all queries and all datasets that fall within the region. We give each dataset equal overall weight in this aggregation, as otherwise LVIS and ObjectNet datasets with 1200 queries and 300 queries respectively would dominate the calculation.

Table 2 shows these average NDCG aggregate. The table also shows the number of queries in each partition. The majority of queries have high NDCG scores, but because we evaluate over 1500 queries, there are still more than 330 queries represented in the low

and medium baseline NDCG areas. Table 2 shows that for those queries SeeSaw improves scores by 3.2 and 2.3 times respectively. For the queries with high initial NDCG we still increase NDCG scores substantially by 17%. Crucially, we do not worsen query results, as a result of the optimizations described in §4 that take special care not to worsen performance when the visual semantic model works well. Finally, we highlight how Figure 2 shows that a number of queries reach an NDCG close to the maximum possible.

Now we move on to breaking down the relative contributions of the two SeeSaw optimizations.

baseline NDCG (# queries)	low (86)	medium (250)	high (1303)
CLIP	.05	.18	.72
this work	.15	.41	.84
ratio	3.22	2.33	1.16

Table 2: Search result accuracy (measured as NDCG) for SeeSaw vs. the baseline implementation. From left to right, each column restricts the evaluation to a subset of queries based on their baseline performance: low means the baseline score was less than .1, and high means the baseline score was greater than .3. SeeSaw offers large NDCG gains on every slice, with the largest gains on those queries for which the model fares poorly, while still improving scores substantially for queries that score high initially.

5.3 User Study

The previous section showed that SeeSaw is able to substantially improve the rate at which relevant objects are found versus a baseline that does not receive feedback. We now present the results of our user study where we evaluate how effective SeeSaw is when real users use our interface to perform search. There are four goals for this user study:

- (1) Measure the end-to-end time required to complete several example search tasks using SeeSaw with real users providing feedback, which can be noisy.
- (2) On the BDD dataset, demonstrate SeeSaw effectiveness on hard queries outside the limited categories of BDD ground-truth data.
- (3) Compare the extra time cost of providing box feedback and the time cost when providing no feedback.

For this evaluation we picked 8 queries over the different datasets and instructed users to conduct these searches. To carry out their searches, Users were randomly assigned either to use SeeSaw or to use the baseline: a stripped-down version of SeeSaw with the same UI, but without requiring or allowing box annotations from them, and without the optimizations from the SeeSaw back-end (§4). In either system users move through returned images using the same keyboard controls. In the control version (the baseline), they can mark a whole image as relevant without drawing a box around it, unlike with SeeSaw.

We recruited 22 users for this study; 10 were research from our university, which we trained and instructed verbally in person. The 12 remaining users were recruited from Amazon Mechanical Turk, for whom we made a video explaining how to carry out the study.

Users were randomly assigned a version of the system they would use. The first query was used to train the users in both the task and the user interface and was omitted from the reported results. In order to keep the user study 30 minutes, including instructions and time between queries, we evaluated only 8 queries, and all users did all queries.

We asked users to search for images containing: A - dogs (BDD), B - wheelchairs (BDD), and C - cars with open doors (BDD), D - melon (COCO) and E - spoons (COCO), the last two, F - dustpans and G - egg cartons were over ObjectNet. Queries A,B, and C do not have labeled ground truth in the BDD dataset, but exemplify more complex queries or rarer situations than available in BDD. Queries D and E are not labeled exhaustively in COCO. Because of this lack of ground truth, we inspected the images shown to the user and user inputs visually after the session to verify results. These queries were selected to be representative of the “low” (A,B,C) and “high” (D,E,F,G) classes in the evaluation presented in Section 5.2, to compare SeeSaw performs with real users on harder and easier objects.

In Figure 3 we show the number of results marked relevant by the user vs. time elapsed for each query. The error bars represent the bootstrapped 95% confidence interval of the median time, and the solid dots the median itself. We highlight the following results: for the first 3 queries (in the BDD dataset) SeeSaw outperforms the baseline by a wide margin. For example, for dogs and wheelchairs, while the initial results are similar for both, it becomes much harder to find them for the baseline (the baseline can find some very prominent dogs, but then cannot find more, and cannot adjust based on the ones found so far). In the case of wheelchairs, the baseline model confuses wheelchair signs with wheelchairs, but the unfortunately the first are far more common in a street setting, users of SeeSaw can help correct this through feedback. For ‘Car with open doors’, initial results are rare on both version of the system, as there are far too many cars with doors, but not many with open doors in the dataset. After finally locating some examples SeeSaw starts picking up on the concept, whereas most users of the baseline failed to find more than 4 examples. We cut off the experiment after 6 minutes and assigned an time value of 6 minutes to users that did not complete it within that time (but in reality this is a lower bound). Queries D, E, F, G, show situations where results are more common; here both versions perform well. While SeeSaw requires feedback, the overhead of the labeling is low enough that that SeeSaw users take about as much time as baseline system users. Note that unlike an object detection labeling task where users must separately label every instance, users can use coarse labels enclosing most of the items of interest, if there are several, which lowers the cost of feedback.

Under both scenarios users may fail to see some of the results. The effect of omission-noise on SeeSaw (which relies on feedback) does not appear large: if one misses the first example of a car with open doors, (which does happen, as it takes around 60 images to get to the first), then the overall time it takes to do the query is longer, but not longer than the baseline.

Latency. The times in Figure 3 include the combined effects of looking at different numbers of images, annotating images, and waiting for the system to return new results. Using the same data from the user study above we also compute the per-frame user

	baseline	seesaw
not marked	1.980 ± .100	2.400 ± .190
marked relevant	3.000 ± .280	4.400 ± .450

Table 3: User annotation time (s) per image depends on whether the image is marked relevant. (2s vs 3s). Localized feedback adds an overhead of about 1.5 seconds per image (4.5s) The \pm denotes the 95% CI.

annotation latency, and show it in Table 3. Because both interfaces require marking images as relevant (either by clicking and drawing a box for SeeSaw or by pressing a key for the baseline), then the time taken for negative images (2s) is shorter than for those marked positive. When marked positive, drawing the box in SeeSaw takes (4.5 s), or 1.5x longer than the baseline (3s), whereas the ratio of accepted to seen images was 1 to 5 in the user study. Hence, when most results are positive for both systems, there is a small added overhead for SeeSaw, which is consistent with Figure 3 for queries F and G. In challenging situations where most results are negative, however, SeeSaw more than compensates for the extra cost. In addition to user-time, we also measured system-time, including vector refinement and lookup times. For the multi-vector representation these costs were on average less than 200 ms, which is not significant compared to user time.

5.4 Optimization breakdown

In this section we break down the individual contributions of the interactive concept refinement §4.1 and pyramid representation §4.2 optimizations. Table 4 shows a breakdown of NDCG scores starting at the top row with a version SeeSaw without either optimization, simply using a visual semantic embedding to search through images (the same as the baseline in the previous section). As in Table 2, we separate queries into the same three groups based on how the visual semantic embedding performs in those groups. On the second row we show how NDCG changes after adding the pyramid representation optimizations. The largest NDCG changes from the pyramid optimization occur in the low and medium tiers of initial performance. Part of the reason is that categories that already do well initially are partially concepts whose corresponding images are already biased to large instances, where results are reasonably easy to spot even at the single image-single vector level, hence the pyramid representation is not as useful and the baseline is already biased toward the right answer by the way the datasets are designed. We highlight however that switching to the pyramid representation does not harm this group despite the noise introduced due to base level pyramid patches, as described in §4.3. and still increases scores a significant amount.

The third row in Table 4 shows NDCG changes after applying concept refinement on top of the pyramid representation optimization. We note both optimizations have about equal contribution to NDCG improvements in all three baseline groups, and that for the medium and low baseline groups, half or more of the total NDCG is due to the combined effect of the optimizations in SeeSaw. In the low baseline group especially, the baseline alone shows the

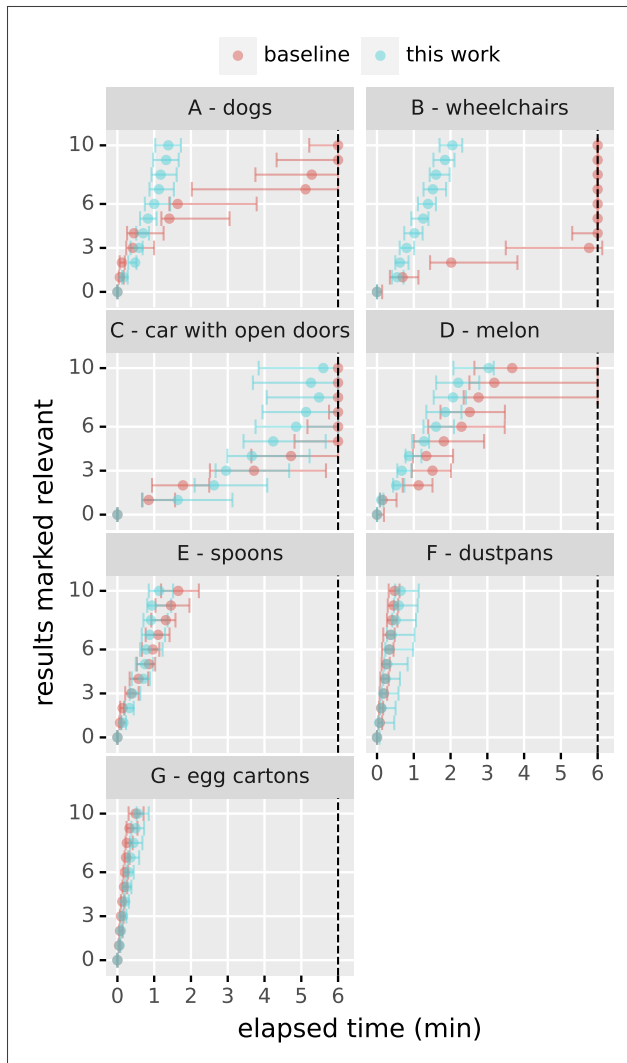


Figure 3: Summary of user study time vs relevant results found for 7 queries. Error bars denote the 95% bootstrapped-CI of the median, and the solid dot is the actual median. We stopped when finding 10 relevant results, or when we hit the 6 minute mark (dashed line). If the error bar lies over the dashed line, it means at least some people failed to find that number of results in the 6 minutes. If the median for a given level lies over the dashed line, then most people failed to reach that number of results.

visual semantic embedding alone can score quite low, and the optimizations in SeeSaw can help substantially improve these scores, enabling users to run searches they would otherwise be unable to carry out.

6 RELATED WORK

In this section we review work related to SeeSaw. Image data present two important challenges from a data management perspective: the first is what interfaces to use to specify queries and the second is what techniques are needed to mitigate the high computational

part variant	.1	.1 delta	.3	.3 delta	1.	1. delta
CLIP	.05		.18		.72	
+ vector pyramid	.08	.03	.35	.17	.76	.05
+ concept refine	.15	.07	.41	.06	.84	.07

Table 4: Cumulative breakdown of contribution of different optimizations in SeeSaw. Queries with low baseline NDCG are those for which the semantic embedding alone has the lowest accuracy. Both the pyramid representation and concept refinement contribute similar amounts of NDCG gain for each category. For those queries with low and medium baseline NDCG, these optimizations contribute the half or more of the NDCG average.

demands of current vision algorithms. Therefore, we organize this section starting with work in related systems that help users *specify* queries on visual datasets including natural language, domain specific languages, and interactive image search systems. Then we describe ‘model-as-specification’ approaches, by which we mean data management techniques that presuppose an accurate but expensive oracle model with structured output and then help reduce the processing costs. Finally, we review work related to the internal implementation of SeeSaw, including existing work on learning to rank and on pyramid representations.

Specifying queries over image datasets There is a large amount of work on image and multimedia search. We focus on recent work.

Rekall[6] provides a domain specific language and data model to help users find custom temporal events in their video data. While targeting video, it is conceivable similar approaches could help handle ad-hoc complex scenes within single images such as ‘person kicking a ball’. Unlike SeeSaw, Rekall’s implementation relies on extracting a representation ahead of time consisting of object boxes and timestamps. Users rely on this base representation to construct and execute ad-hoc queries, but these queries can only specify object types the pre-trained object detector knows about. Thus, an approach like SeeSaw could be used as a way to extend composition based approaches like Rekall. There are other systems that rely on having a bounding boxes available to then help process video queries, such as MIRIS[3].

Interactive Image Search and Content Based Image Retrieval. The information retrieval community has worked on the problem of interactive image search, or so-called *content-based image retrieval* [16, 25]. Early instances of this work were done in a web search setting, where search is driven by the context in which an image appears, e.g., the words around the image on a page, or by using simple image features such as color histograms. More recent work from the computer vision community has looked at using embeddings to find similar images, with great success in applications such as facial recognition [20]. However, such work is not focused on interactive search but on finding an image similar to a target image. More recent work from the machine learning community has worked on interactive search using user-feedback in the form of text [22], but has assumed that images are pre-processed with an object detector trained to detect a fixed taxonomy of objects, unlike SeeSaw which is designed to find new, previously detected object types in an image database.

Model-as-specification approaches. One recent line of work related to image data querying is based on assuming users can access an accurate but potentially expensive model to answer a query, where the goal is to reduce the cost and time of to answer queries over images. To do this, prior work has developed many different learning-to-approximate techniques that use lightweight models to approximate the reference model, using the reference model as supervision. This includes work in [12],[11], and more recently [13]. This is quite different than SeeSaw, where the goal is to optimize search queries only, without a reference model at all (i.e., SeeSaw finds new classes of objects for which no reference model is available.). Work such as Chameleon[9] aims to reduce model-inference costs as well, but also assumes there is a reference model available.

6.1 Implementation related work

Learning to rank. The pairwise hinge loss formulation of learning to rank §4.1 dates back to at least [10], done in the context of web-search. Since then, this type of ranking loss function based on pairs has been used widely for retrieval tasks, for example for face similarity embeddings[20]. In SeeSaw we do not train a deep ranking model or embedding from scratch. The specific problem in SeeSaw is developing a coherent method to merge the initial search vector derived from a user search string with the user feedback quickly on every batch. SeeSaw uses the same loss function as a starting point to derive a formula for this update because pairwise loss functions naturally handle different degrees of imbalance between positive and negative examples, which are common in the use cases SeeSaw handles and change from iteration to iteration.

Pyramid representations. The idea of image representations consisting of progressively downscaled versions of the same image goes back many decades[1]. The current generation of object detectors such as MaskRCNN[8] also incorporate some pyramid ideas in their architectures but avoid processing multiple replicas of the same image like SeeSaw does partly due to cost [15]. Unlike SeeSaw however, they can rely on training to help handle multiple scales and assume they will run on very similar data. SeeSaw re-uses the pyramid representations across many searches, so it is more feasible to use the full pyramid. Further, SeeSaw has to manage the specific noise issues described in §4.3 without prior training.

Data augmentation. Multiscale averaging of vectors §4.3.1 is related to test-time augmentation. There are several key differences with typical test time augmentation, the first is cost: SeeSaw already computed feature vectors at the cost of employing patches that do not perfectly align around the region of interest. This choice keeps the computation lightweight and lets us re-score a potentially large short-list of hundreds of different images. For typical test-time augmentation outside of SeeSaw, the full deep net is run on multiple versions of the same image that was altered in multiple ad-hoc ways. This type of augmentation increases costs substantially. The second difference is Multi-scale averaging is not an ad-hoc optimization in SeeSaw but a fix that addresses the extra false positives by the large number of fine-grained vectors and their large score variance compared to those of coarser levels in the pyramid. The underlying principle of attempting to reduce the variance component of error by averaging is similar in both situations.

7 CONCLUSION

We presented SeeSaw, an interactive system for ad-hoc search over image datasets. SeeSaw helps users specify and refine searches for objects or scenes of interest within their image datasets. SeeSaw’s interface leverages natural language and user annotations in the form of bounding boxes around regions of interest. SeeSaw introduces two techniques to help translate this user feedback into a better set of results in the next iteration: interactive concept refinement and pyramid representation. These techniques enable users and SeeSaw work in a loop to refine the query and to manage situations where the embedding models SeeSaw relies on for search fall short in accuracy. SeeSaw gives users a way to find results even for rare categories not served well by available external models. We evaluated SeeSaw against a strong search baseline based on CLIP, a state of the art visual-semantic embedding, and show SeeSaw boosts search accuracy for most queries in a comprehensive benchmark of thousands of different queries, boosting NDCG score by an average of 4.1x on the queries where the pre-trained embeddings perform poorly, and substantially on almost all queries, even those where CLIP does well.

REFERENCES

- [1] Edward Adelson, Charles Anderson, James Bergen, Peter Burt, and Joan Ogden. 1983. Pyramid Methods in Image Processing. *RCA Eng.* 29 (11 1983).
- [2] Andrei Barbu, David Mayo, Julian Alverio, William Luo, Christopher Wang, Dan Gutfreund, Josh Tenenbaum, and Boris Katz. 2019. ObjectNet: A large-scale bias-controlled dataset for pushing the limits of object recognition models. In *Advances in Neural Information Processing Systems*, H Wallach, H Larochelle, A Beygelzimer, F Alché-Buc, E Fox, and R Garnett (Eds.), Vol. 32. Curran Associates, Inc.
- [3] Favyen Bastani, Songtao He, Arjun Balasingam, Karthik Gopalakrishnan, Mohammad Alizadeh, Hari Balakrishnan, Michael Cafarella, Tim Kraska, and Sam Madden. 2020. MIRIS: Fast Object Track Queries in Video. In *Proceedings of the 2020 ACM SIGMOD International Conference on Management of Data* (Portland, OR, USA) (*SIGMOD '20*). Association for Computing Machinery, New York, NY, USA, 1907–1921. <https://doi.org/10.1145/3318464.3389692>
- [4] E. Bernhardtsson. [n.d.]. ANNOY: Approximate Nearest Neighbors Oh Yeah. <https://github.com/spotify/annoy>. Accessed: 2021-05-20.
- [5] Ting-Wu Chin, 1. Ruizhou Ding, and 1. Diana Marculescu. [n.d.]. ADASCALE: TOWARDS REAL-TIME VIDEO OBJECT DETECTION USING ADAPTIVE SCALING. ([n.d.]).
- [6] Daniel Y. Fu, Will Crichton, James Hong, Xinwei Yao, Haotian Zhang, Anh Truong, Avani Narayan, Maneesh Agrawala, Christopher Ré, and Kayvon Fatahalian. 2019. Recall: Specifying Video Events using Compositions of Spatiotemporal Labels. (Oct 2019). <http://arxiv.org/abs/1910.02993>
- [7] Agrim Gupta, Piotr Dollár, and Ross Girshick. 2019. LVIS: A Dataset for Large Vocabulary Instance Segmentation. *arXiv [cs.CV]* (Aug 2019). <https://arxiv.org/abs/1908.03195>
- [8] Kaiming He, Georgia Gkioxari, Piotr Dollár, and Ross B. Girshick. 2017. Mask R-CNN. *CoRR abs/1703.06870* (2017). arXiv:1703.06870 <http://arxiv.org/abs/1703.06870>
- [9] Junchen Jiang, Ganesh Ananthanarayanan, Peter Bodik, Siddhartha Sen, and Ion Stoica. 2018. Chameleon: scalable adaptation of video analytics. In *Proceedings of the 2018 Conference of the ACM Special Interest Group on Data Communication*, Vol. 4. ACM, 253–266.
- [10] Thorsten Joachims. 2002. Optimizing search engines using clickthrough data. In *Proceedings of the eighth ACM SIGKDD international conference on Knowledge discovery and data mining - KDD '02*. ACM Press. <https://doi.org/10.1145/775066.775067>
- [11] Daniel Kang, Peter Bailis, and Matei Zaharia. 2018. BlazeIt: Fast Exploratory Video Queries using Neural Networks. *CoRR abs/1805.01046* (2018). arXiv:1805.01046 <http://arxiv.org/abs/1805.01046>
- [12] Daniel Kang, John Emmons, Firas Abuzaid, Peter Bailis, and Matei Zaharia. 2017. NoScope: Optimizing Neural Network Queries over Video at Scale. *Proc. VLDB Endow.* 10, 11 (Aug. 2017), 1586–1597. <https://doi.org/10.14778/3137628.3137664>
- [13] Daniel Kang, John Guibas, Peter Bailis, Tatsunori Hashimoto, and Matei Zaharia. 2020. Task-agnostic Indexes for Deep Learning-based Queries over Unstructured Data. (Sep 2020). <http://arxiv.org/abs/2009.04540>
- [14] Tsung-Yi Lin, Michael Maire, Serge J. Belongie, Lubomir D. Bourdev, Ross B. Girshick, James Hays, Pietro Perona, Deva Ramanan, Piotr Dollár, and C. Lawrence Zitnick. 2014. Microsoft COCO: Common Objects in Context. *CoRR abs/1405.0312* (2014). arXiv:1405.0312 <http://arxiv.org/abs/1405.0312>
- [15] Tsung-Yi Lin, Piotr Dollár, Ross Girshick, Kaiming He, Bharath Hariharan, and Serge Belongie. 2016. Feature Pyramid Networks for Object Detection. (Dec 2016). <http://arxiv.org/abs/1612.03144>
- [16] Ying Liu, Dengsheng Zhang, Guojun Lu, and Wei-Ying Ma. 2007. A survey of content-based image retrieval with high-level semantics. *Pattern recognition* 40, 1 (2007), 262–282.
- [17] C.D. Manning, P. Raghavan, and H. Schütze. 2008. *Introduction to Information Retrieval*. Cambridge University Press. <https://books.google.com/books?id=t1PoSh4uwVcC>
- [18] F. Pedregosa, G. Varoquaux, A. Gramfort, V. Michel, B. Thirion, O. Grisel, M. Blondel, P. Prettenhofer, R. Weiss, V. Dubourg, J. Vanderplas, A. Passos, D. Cournapeau, M. Brucher, M. Perrot, and E. Duchesnay. 2011. Scikit-learn: Machine Learning in Python. *Journal of Machine Learning Research* 12 (2011), 2825–2830.
- [19] Alec Radford, 1. Jong Wook Kim, 1. Chris Hallacy, Aditya Ramesh, Gabriel Goh, Sandhini Agarwal, Girish Sastry, Amanda Askell, Pamela Mishkin, Jack Clark, and et al. [n.d.]. Learning transferable visual models from natural language supervision. https://cdn.openai.com/papers/Learning_Transferable_Visual_Models_From_Natural_Language_Supervision.pdf
- [20] Florian Schroff, Dmitry Kalenichenko, and James Philbin. 2015. FaceNet: A unified embedding for face recognition and clustering. In *2015 IEEE Conference on Computer Vision and Pattern Recognition (CVPR)*. 815–823. <https://doi.org/10.1109/CVPR.2015.7298682>
- [21] Amanpreet Singh, Vedanuj Goswami, Vivek Natarajan, Yu Jiang, Xinlei Chen, Meet Shah, Marcus Rohrbach, Dhruv Batra, and Devi Parikh. 2020. MMF: A multimodal framework for vision and language research. <https://github.com/facebookresearch/mmf>.
- [22] Fuwen Tan, Paola Cascante-Bonilla, Xiaoxiao Guo, Hui Wu, Song Feng, and Vicente Ordonez. 2019. Drill-down: Interactive Retrieval of Complex Scenes using Natural Language Queries. In *Advances in Neural Information Processing Systems 32: Annual Conference on Neural Information Processing Systems 2019, NeurIPS 2019, December 8-14, 2019, Vancouver, BC, Canada*, Hanna M. Wallach, Hugo Larochelle, Alina Beygelzimer, Florence d’Alché-Buc, Emily B. Fox, and Roman Garnett (Eds.). 2647–2657.
- [23] Hugo Touvron, Andrea Vedaldi, Matthijs Douze, and Herve Jegou. 2019. Fixing the train-test resolution discrepancy. In *Advances in Neural Information Processing Systems*, H. Wallach, H. Larochelle, A. Beygelzimer, F. d’Alché-Buc, E. Fox, and R. Garnett (Eds.), Vol. 32. Curran Associates, Inc. <https://proceedings.neurips.cc/paper/2019/file/d03a857a23b5285736c4d5e0bb067c8-Paper.pdf>
- [24] Fisher Yu, Wenqi Xian, Yingying Chen, Fangchen Liu, Mike Liao, Vashisht Mahdavan, and Trevor Darrell. 2018. BDD100K: A Diverse Driving Video Database with Scalable Annotation Tooling. *CoRR abs/1805.04687* (2018). arXiv:1805.04687 <http://arxiv.org/abs/1805.04687>
- [25] Wengang Zhou, Houqiang Li, and Qi Tian. 2017. Recent advance in content-based image retrieval: A literature survey. *arXiv preprint arXiv:1706.06064* (2017).